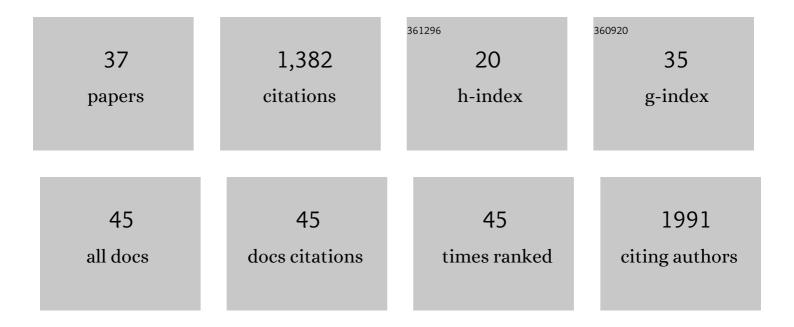
## Suman De

List of Publications by Year in descending order

Source: https://exaly.com/author-pdf/7982786/publications.pdf Version: 2024-02-01



SUMAN DE

	Alpha synuclein aggregation drives ferroptosis: an interplay of iron, calcium and lipid peroxidation.		
1	Cell Death and Differentiation, 2020, 27, 2781-2796.	5.0	142
2	Different soluble aggregates of Aβ42 can give rise to cellular toxicity through different mechanisms. Nature Communications, 2019, 10, 1541.	5.8	140
3	Hsp70 Inhibits the Nucleation and Elongation of Tau and Sequesters Tau Aggregates with High Affinity. ACS Chemical Biology, 2018, 13, 636-646.	1.6	96
4	Ultranarrow and Widely TunableMn2+-Induced Photoluminescence from Single Mn-Doped Nanocrystals of ZnS-CdS Alloys. Physical Review Letters, 2013, 110, 267401.	2.9	84
5	Mapping Surface Hydrophobicity of α-Synuclein Oligomers at the Nanoscale. Nano Letters, 2018, 18, 7494-7501.	4.5	83
6	Ultrasensitive Measurement of Ca <sup>2+</sup> Influx into Lipid Vesicles Induced by Protein Aggregates. Angewandte Chemie - International Edition, 2017, 56, 7750-7754.	7.2	72
7	Soluble aggregates present in cerebrospinal fluid change in size and mechanism of toxicity during Alzheimer's disease progression. Acta Neuropathologica Communications, 2019, 7, 120.	2.4	64
8	Plasticization of Poly(vinylpyrrolidone) Thin Films under Ambient Humidity: Insight from Single-Molecule Tracer Diffusion Dynamics. Journal of Physical Chemistry B, 2013, 117, 7771-7782.	1.2	62
9	Single-Molecule Characterization of the Interactions between Extracellular Chaperones and Toxic α-Synuclein Oligomers. Cell Reports, 2018, 23, 3492-3500.	2.9	59
10	Nanoscopic Characterisation of Individual Endogenous Protein Aggregates in Human Neuronal Cells. ChemBioChem, 2018, 19, 2033-2038.	1.3	52
11	Two Distinct Origins of Highly Localized Luminescent Centers within InGaN/GaN Quantumâ€Well Lightâ€Emitting Diodes. Advanced Functional Materials, 2011, 21, 3828-3835.	7.8	45
12	Spectrally Resolved Photoluminescence Imaging of ZnO Nanocrystals at Single-Particle Levels. Journal of Physical Chemistry Letters, 2011, 2, 1241-1247.	2.1	43
13	Quantum-confined stark effect in localized luminescent centers within InGaN/GaN quantum-well based light emitting diodes. Applied Physics Letters, 2012, 101, .	1.5	40
14	Optical Structural Analysis of Individual α‣ynuclein Oligomers. Angewandte Chemie - International Edition, 2018, 57, 4886-4890.	7.2	40
15	Quantifying Co-Oligomer Formation by α-Synuclein. ACS Nano, 2018, 12, 10855-10866.	7.3	38
16	Direct measurement of lipid membrane disruption connects kinetics and toxicity of Aβ42 aggregation. Nature Structural and Molecular Biology, 2020, 27, 886-891.	3.6	38
17	Wild-type sTREM2 blocks AÎ <sup>2</sup> aggregation and neurotoxicity, but the Alzheimer's R47H mutant increases AÎ <sup>2</sup> aggregation. Journal of Biological Chemistry, 2021, 296, 100631.	1.6	33
18	Soluble amyloid beta-containing aggregates are present throughout the brain at early stages of Alzheimer's disease. Brain Communications, 2021, 3, fcab147.	1.5	32

SUMAN DE

#	Article	IF	CITATIONS
19	Developmentally Regulated GTP binding protein 1 (DRG1) controls microtubule dynamics. Scientific Reports, 2017, 7, 9996.	1.6	26
20	Direct observation of prion protein oligomer formation reveals an aggregation mechanism with multiple conformationally distinct species. Chemical Science, 2019, 10, 4588-4597.	3.7	22
21	Analysis of α-synuclein species enriched from cerebral cortex of humans with sporadic dementia with Lewy bodies. Brain Communications, 2020, 2, fcaa010.	1.5	21
22	Hyperphosphorylated tau self-assembles into amorphous aggregates eliciting TLR4-dependent responses. Nature Communications, 2022, 13, 2692.	5.8	21
23	Inhibiting the Ca 2+ Influx Induced by Human CSF. Cell Reports, 2017, 21, 3310-3316.	2.9	20
24	Increased Secondary Nucleation Underlies Accelerated Aggregation of the Four-Residue N-Terminally Truncated Aβ42 Species Aβ5–42. ACS Chemical Neuroscience, 2019, 10, 2374-2384.	1.7	16
25	Imaging individual protein aggregates to follow aggregation and determine the role of aggregates in neurodegenerative disease. Biochimica Et Biophysica Acta - Proteins and Proteomics, 2019, 1867, 870-878.	1.1	15
26	Tumour necrosis factor induces increased production of extracellular amyloid-β- and α-synuclein-containing aggregates by human Alzheimer's disease neurons. Brain Communications, 2020, 2, fcaa146.	1.5	14
27	Optoelectronic behaviors and carrier dynamics of individual localized luminescent centers in InGaN quantum-well light emitting diodes. Applied Physics Letters, 2011, 99, .	1.5	13
28	Structure-specific amyloid precipitation in biofluids. Nature Chemistry, 2022, 14, 1045-1053.	6.6	11
29	Heterogeneity during Plasticization of Poly(vinylpyrrolidone): Insights from Reorientational Mobility of Single Fluorescent Probes. Journal of Physical Chemistry B, 2016, 120, 12404-12415.	1.2	9
30	Ultrasensitive Measurement of Ca <sup>2+</sup> Influx into Lipid Vesicles Induced by Protein Aggregates. Angewandte Chemie, 2017, 129, 7858-7862.	1.6	9
31	Custom-Made Microspheres for Optical Tweezers. Methods in Molecular Biology, 2017, 1486, 137-155.	0.4	7
32	Heterogeneity in optical properties of near white-light emissive europium complex species revealed by spectroscopy of single nanoaggregates. Chemical Physics Letters, 2017, 667, 247-253.	1.2	4
33	An approach to estimate spatial distribution of analyte within cells using spectrally-resolved fluorescence microscopy. Methods and Applications in Fluorescence, 2017, 5, 014003.	1.1	2
34	[P3–074]: AN ULTRA‧ENSITIVE ASSAY TO MEASURE AGGREGATE INDUCED CA <sup>2+</sup> INFLUX IN HUMAN CEREBROSPINAL FLUID. Alzheimer's and Dementia, 2017, 13, P960.	0.4	1
35	Light-Emitting Diodes: Two Distinct Origins of Highly Localized Luminescent Centers within InGaN/GaN Quantum-Well Light-Emitting Diodes (Adv. Funct. Mater. 20/2011). Advanced Functional Materials, 2011, 21, 3827-3827.	7.8	0
36	Optical Structural Analysis of Individual α‣ynuclein Oligomers. Angewandte Chemie, 2018, 130, 4980-4984.	1.6	0

#	Article	IF	CITATIONS
37	Fast 3D imaging of giant unilamellar vesicles using reflected lightâ€sheet microscopy with single molecule sensitivity. Journal of Microscopy, 2021, 285, 40.	0.8	Ο